# What is the reason for the high Bouguer gravity anomaly at Çumra, Konya (Central Anatolia)?

**Nedim Gökhan AYDIN\***, **Turgay İŞSEVEN**

Department of Geophysical Engineering, Faculty of Mines, İstanbul Technical University, İstanbul, Turkey

**Abstract:** The Bouguer gravity anomaly map of Turkey shows relatively high values around the Çumra region, Konya. This area has a flat topography and a thick cover of sediments despite being seated on a suture zone formed between Anatolide and Tauride Platforms after the Neo-Tethys Ocean closed. High Bouguer gravity anomalies indicate an anomalous mass excess buried under the flat topography. In the present study, the gravity anomaly is studied using several analysis and processing methods in order to understand and infer its possible sources. Spectral analysis of the anomaly showed that the mass should be buried at a depth of about 4.8 km. The geometry of the mass is forward modelled using the vertical prisms method, which assumes that the mass is a homogeneous layer, represented by separate identical prisms. The observed anomaly and the calculated anomaly retrieved from the modelled geometry are compared mathematically and the mass geometry is updated depending on the differences between them. After a total of 10 iterations, the RMS error decreases below 1% and thus the calculated model is considered accurate. Then the achieved model is used for mass estimations, which showed that if the density difference between the medium and the target mass is set as 0.25 g/cm³, about 67 Gt of extra mass is needed to produce such a gravity anomaly. Correlation with geological maps and aeromagnetic anomalies of the region points out that this excess mass may be due to a remnant ophiolitic rock from the Neo-Tethys Ocean.

**Key words:** Gravity, Konya, Bouguer, spectral analysis, vertical prisms modelling, Tethys, obduction

## 1. Introduction

The Gravity method tracks gravitational acceleration depending on displacement and uses the gravity data to estimate underground density distribution with several analysis and filtering processes. The aim of the present study was to investigate the reason for high Bouguer gravity anomalies from the Çumra region, Konya. The study area, shown in Figure 1, lies on a suture zone at the southwestern edge of the Kırşehir Massif in Central Anatolia (Okay and Tüysüz, 1999). Despite the existence of ophiolitic rocks in the region, the Bouguer anomalies show relatively high values above the Konya Basin, which is covered with a thick layer of sediments. The high Bouguer gravity values in the study area can be explained by a large buried mass with a higher density than its surroundings.

The planned modelling method is the vertical prisms method (Cordell and Henderson, 1968), which has previously been applied by Kearey (1991), Ateş and Kearey (1995), and Büyüksaraç et al. (1998). For this purpose, new computer software called GravPack is written in MATLAB to handle gridding, spectral analysis, filtering, and modelling processes.

Scattered gravity data are firstly gridded with cubic spline interpolation using the software. Then the power spectrum of the Bouguer anomalies is calculated to estimate an initial depth for the model using Spector and Grant's (1970) approximation in the same way as described in the literature (Hahn et al., 1976; Maus and Dimri, 1996; Nouck et al., 2006). In order to decrease the effects of masses seated at shallower depths, the Bouguer anomaly data are filtered using low pass filters, the cutting wavenumber of which is picked from the power spectrum plot. The filtered Bouguer anomaly grid is used as the input data for the vertical prisms method to retrieve a mass distribution model that would cause the measured gravity anomalies. Finally, the results are discussed considering ophiolitic rock distributions, aeromagnetic anomalies, and the complex geological history of the study area.

## 2. Geology of the Çumra region

Anatolia has a complex geologic setting since it is located where the Paleo-Tethys and the Neo-Tethys Oceans are closed (Robertson et al., 2009). The Paleo-Tethys Ocean closed during the Mid-Jurassic period, due to spread of
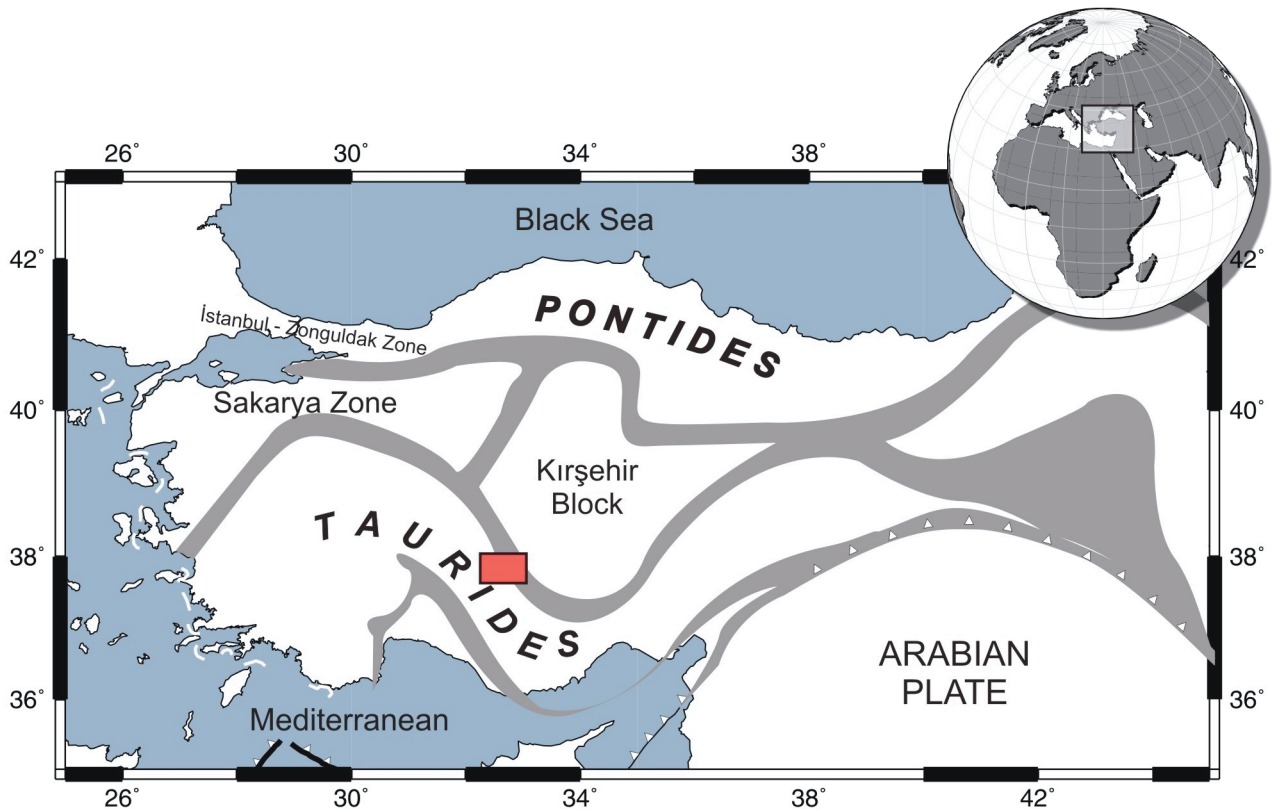
---

\* Correspondence: aydinn@itu.edu.tr

**Figure 1.** Paleotectonic units of Turkey (Okay and Tüysüz, 1999). Red box shows the study area.

the Atlantic Ocean (Smith, 1971; Dewey and Burke, 1973). Later, the continents were uplifted, carbonate sediments were accumulated, and Neo-Tethys ophiolites were formed reaching the Lower-Cretaceous period (Şengör and Yılmaz, 1981). During the Upper Cretaceous period, the oceanic crust started to subduct towards the north alongside the southern part of the Pontide belt, thus leading to harsh volcanic activities and the reposition of ophiolites over the Anatolide–Tauride platform (Okay, 2011). During the Lower Miocene period, the Arabian and Eurasian plates collided, the Neo-Tethys Ocean closed, and the tectonic structures that are now seen in Turkey started to form during the Mid-Miocene period (Okay, 2008).

The geological map of the study area (simplified from MTA (2002)) shows that the area is mostly covered with carbonate-related sediments (Figure 2). There are also volcanic rocks and ophiolites in places, which is expected considering the area is a suture zone (Okay and Tüysüz, 1999). Large bodies of Paleozoic–Cretaceous marble formations can be seen in the north, northwest, southwest, and southeast parts of the study area, most of which appears to be covered with younger sediments. In the west and south parts of the area, volcanic rocks appear along with smaller-sized ophiolitic bodies. Most of the area

is covered with young carbonates, aged between Mid-Miocene and Quaternary.

## 3. Data and methodology

The study area covers an area of $110 \times 132$ km$^2$, with a high Bouguer anomaly at the center (Figure 3). The Bouguer gravity data of the study area are digitized from the Bouguer Gravity Anomaly Map of Turkey (MTA, 2006). More than 100 arbitrary points are carefully picked from the map to preserve the anomalies. The data are then resampled into a $111 \times 133$ data grid with 1-km sampling rate using the cubic interpolation method, in order to increase the resolution of the resulting model. The Bouguer Gravity Map of Turkey is projected on the Lambert plane with decimal degree coordinates. Since the vertical prisms method uses kilometers as distance units, the Bouguer data for the Çumra area are converted into UTM coordinates with the WGS84 datum.

The Bouguer anomaly of the region ranges from –100 to –10 mGal (Figure 3). The lowest values (–100 to –70 mGal) are located between Konya, Başhüyük, Derbent, and the west of Akören, and appeared to be over late Paleozoic to early Jurassic metamorphic rock masses and some parts of lower Cretaceous sedimentary rocks. The
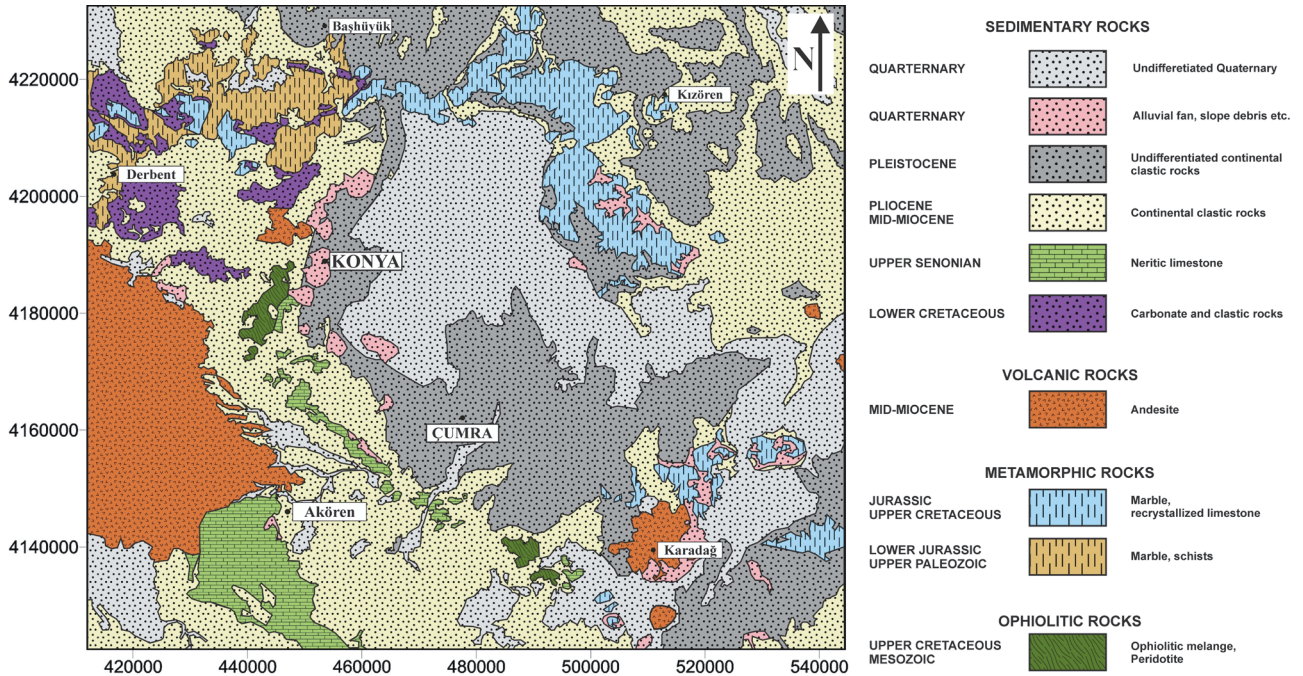
**Figure 2.** Geology map of Konya (Çumra) and surrounding area. Simplified from MTA (2002).
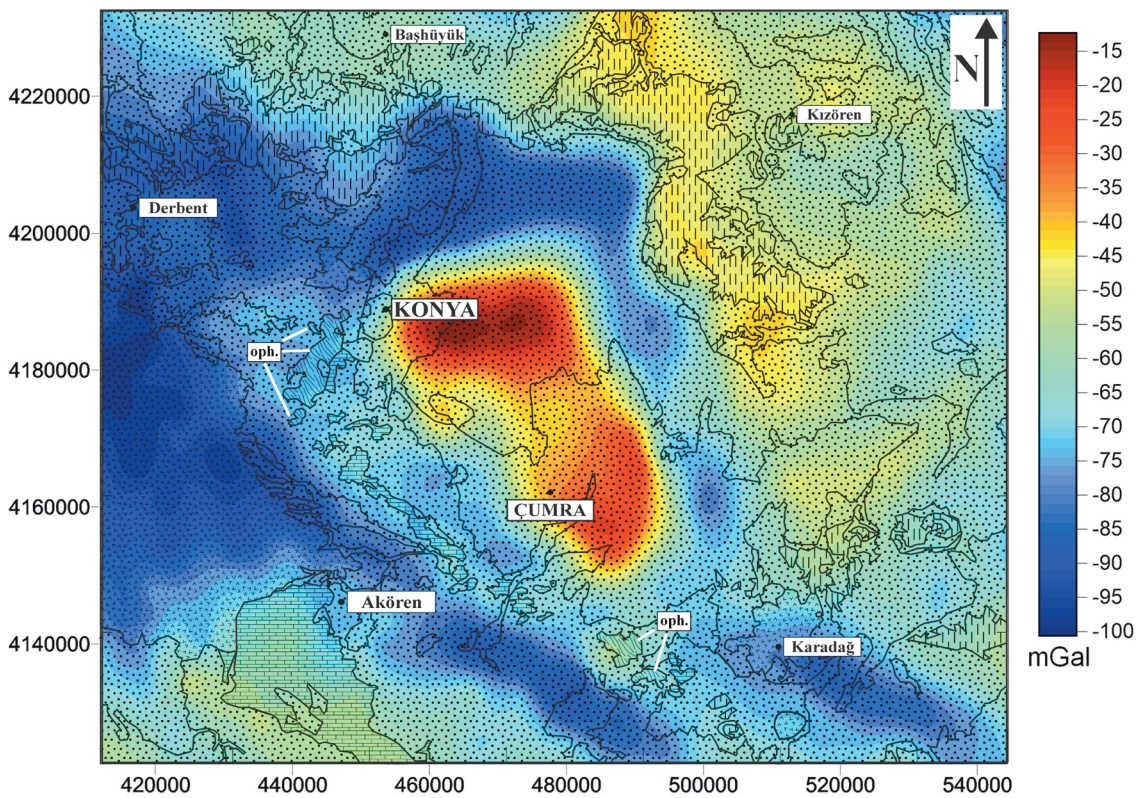


**Figure 3.** Bouguer anomaly map is overlapped with the geology map (MTA, 2002). Lowest Bouguer values (dark blue-blue) mark sediments and volcanics. Mid-range values (cyan-yellow) mostly mark limestones and marbles. Highest ones (orange red) located over sediments at the center. oph. shows ophiolite outcrops.

NW–SE directed ophiolitic alignment following the suture zone given in Figure 1 can be seen along a low Bouguer anomaly ensemble around Akören. There are Paleozoic and Jurassic–Cretaceous marbles and recrystallized limestone to the north, northeast, and east of Konya, matching the Bouguer anomaly map and covering most of the anomalies between –70 and –45 mGal. There are also upper Senonian neritic limestones surfaced around Akören with Bouguer anomalies between –75 and –55 mGal. To the west of Konya, there are Mid-Miocene andesites marked between –100 and –60 mGal anomaly values. To the southeast of Konya and north of Çumra, there are relatively high Bouguer values (–35 to –15 mGal) despite the area having a flat topography and being covered with Cretaceous clastic sediments.

The high Bouguer values over the Konya Basin may be due to an excess of mass or an uplift of a high density layer, both of which are buried under the sediments. In the present study, firstly, we assumed a theoretical anomalous layer under the Konya Basin and estimated its geometry using the vertical prisms method (Cordell and Henderson, 1968). Secondly, the theoretical model was used to approximate the amount of buried mass that would result in the observed Bouguer anomalies.

This method assumes underground structures composed of adjacent and vertical prisms, calculates the gravity anomaly separately for each of these prisms, and sums all of the obtained results for each point defined on the Earth's surface (Öksüm et al., 2005). The height of each prism represents the layer's depth for its position, which could be estimated using Eq. (1) with a nonnegligible amount of error (Genç, 1997). This equation is used to achieve an initial model for the layer at depth, which is assumed to be separated into vertical prisms.

$$\Delta g_p = 2\pi G \rho \Delta z_i \quad (1)$$

For the point $(x', y', z')$ on the Earth's surface, the gravitational acceleration contribution of a prism defined between $(x_1, y_1, z_1)$ and $(x_2, y_2, z_2)$ points with a density difference of $\Delta\rho$ can be calculated in terms of the coordinate system defined in Figure 4a using Eq. (2). Prisms are placed beneath the surface so that the horizontal center of the prisms would coincide with the gridded data points on the surface, thus making the width of the prisms the same as the gridding interval (Figure 4b). The R parameter in Eq. (2) defines the distance between the data point and the corners of the prism in kilometers (Eq. (3)). Since the prisms are in this way geometrically defined, it is possible to calculate each prism's contribution to the total gravitational acceleration at any given point. Calculating the gravitational acceleration contribution of each prism for each point at the surface will result in a theoretical Bouguer anomaly.

$$\Delta g(x', y', z') =$$

$$-G\Delta\rho \left[\left[\left[(x-x')\times\ln(y-y'+R)\right.\right.\right.$$
$$+ (y-y')\times\ln(x-x'+R)$$
$$\left.\left.\left.+ z\arctan\left(z\times\frac{R}{(x-x')(y-y')}\right)\right]_{x_1}^{x_2}\right]_{y_1}^{y_2}\right]_{z_1}^{z_2} \quad (2)$$

$$R = \sqrt{(x-x')^2 + (y-y')^2 + (z-z')^2} \quad (3)$$

Modelling processes are carried out over a selected and limited part of the Earth, which means all the data and gravitational contribution outside the limited area is neglected. This would result in data loss on the sides of the study area during the modelling process. Including a fair
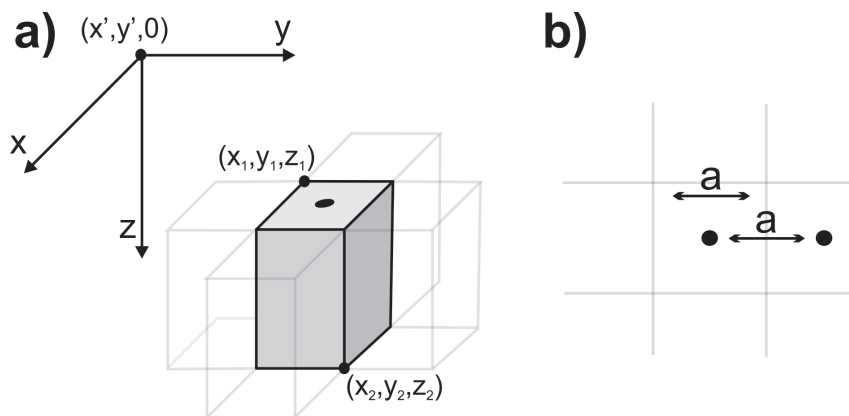


**Figure 4.** Geometrical definitions of prisms in the vertical prisms method. a) Coordinate system of prisms in Eqs. (2) and (3). b) Placement of prisms over data points on grid.

amount of mass effect that is outside the modelling area into the calculations could not remove the loss completely, but would decrease its effect drastically (Figure 5). For this purpose, all the prisms that are located at the edges and at the corners of the modelling area are assumed to be extended outwards from the area. The extension amount could be optional, but a trial and error process showed that extending half of the modelling area gives acceptable results. In this way, the extra included mass would not be constant or random, but would depend on the calculated model and the modelling area itself.

After an initial depth model is achieved using Eq. (1) and the theoretical gravity anomaly of the initial model is calculated using Eqs. (2) and (3), these anomalies are compared by calculating the error. Instead of following general inverse solution methods, the inverse solution of the vertical prisms method is applied for each prism and data point separately. The depth model is updated comparing observed and theoretical anomalies for each point. The amount of change in prisms' heights could be estimated using Eq. (1) for each prism, depending on the differences between the two anomalies. Iterating with this process would decrease the differences between observed and theoretical anomalies, which could be monitored calculating root mean square (RMS) errors.

## 4. Depth estimation by spectral analysis

The gravity method depends on the density, geometry, and depth of underground masses. In order to carry out a modelling process with one of these parameters, the two other parameters should be fixed. This study focuses on a certain geometry layer with homogeneous properties for the modelling process; thus the density difference and the average depth parameters were required to be fixed at constant values (Figure 6). The density difference ($\Delta\rho$) can be defined considering the information about the geology and Bouguer data. For the average depth estimation, spectral analysis data of the Bouguer anomalies can be used (Spector and Grant, 1970).

Spectral analysis of the Bouguer data is carried out by calculating the radially averaged power spectrum of the data in the Fourier domain. First, the 2D fast Fourier transform of the anomaly is computed. Then the transformed data are divided into circles starting from the center and the radii of circles increase in equal steps. All the points between these circular intervals are averaged and squared to calculate power spectrums. Analysis would return exponential amplitudes and values of wavenumber for corresponding circle radii (Spector and Grant, 1970; Parker, 1972).
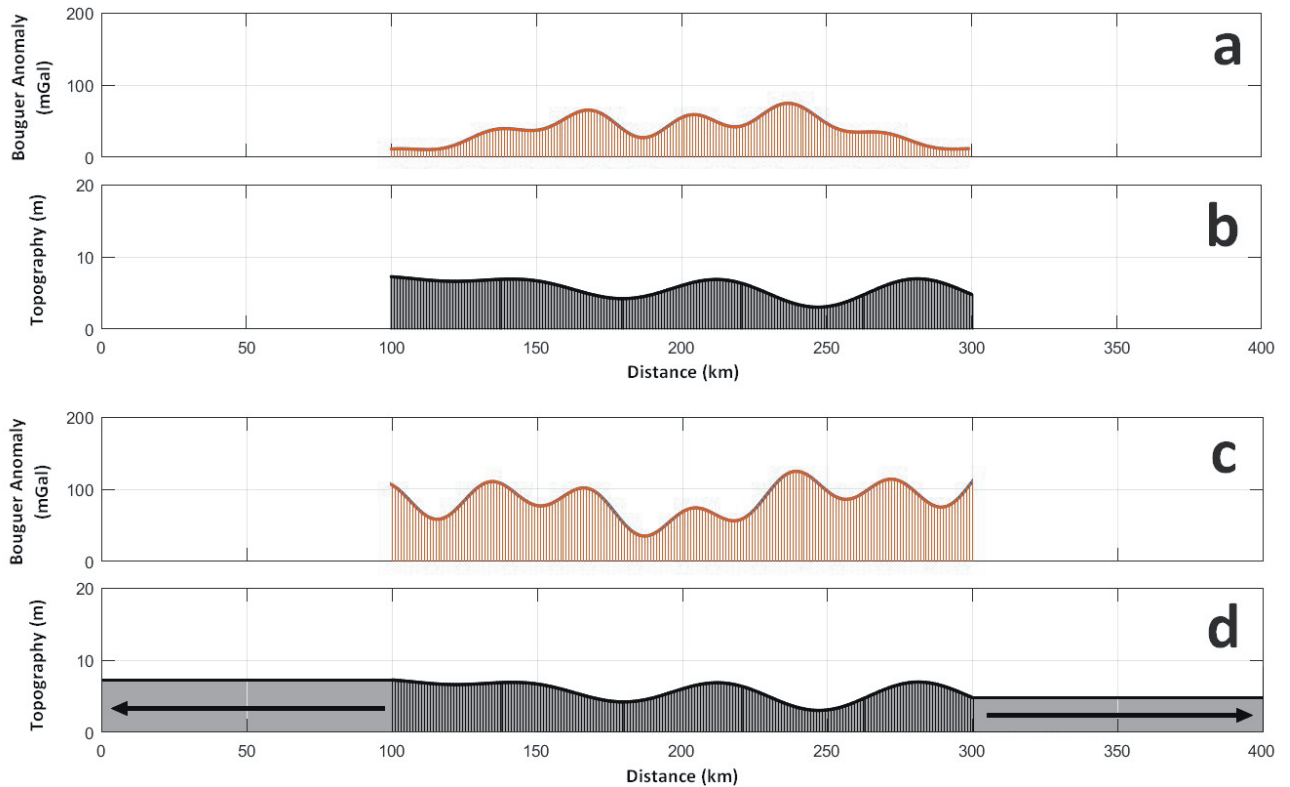


**Figure 5.** Two-dimensional explanation of data loss on the sides during the modelling process. Bouguer anomalies result in data loss (a) for limited topography (b). The data loss is decreased (c) for outwards extended topography (d).
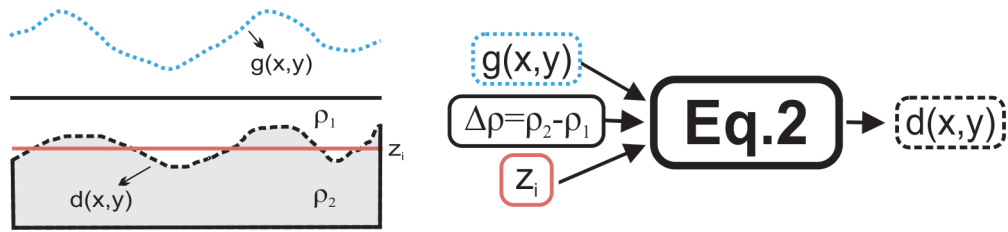
**Figure 6.** A simple slice model and chart displaying the modelling parameters. Gravity data g(x,y) (blue line), initial depth $z_i$ (red line), and density difference ($\Delta\rho$) parameters are fixed and used in Eq. (2) to calculate the depth model d(x,y) (dashed line).

Plotting the power spectrum would reveal the effects of different layers within an anomaly, appearing as linear alignments between certain wavenumber values. Spector and Grant (1970) noted that the slopes of these alignments have a relation with approximate layer depths and it is possible to estimate average depths of these layers using line fitting equations (Banks and Swain, 1978; Pawlowski and Hansen, 1990). GravPack calculates the depth estimation using Eq. (4).

$$h = \frac{-(\ln(\tilde{E}_2) - \ln(\tilde{E}_1))}{2\pi(k_2 - k_1)} \tag{4}$$

Spectral analysis approximations would be useful in calculations since the vertical prisms method requires an average depth value to be iterated for the correct geometry.

## 5. Modelling

The power spectrum of the Çumra Bouguer anomaly is computed using the written MATLAB software, GravPack. On the power spectrum, there are two visible linear alignments up to 0.6 rad/km (Figure 7). In the present study, the first linear alignment on the lowest wavenumber values (including first 9 points) is used for depth estimation, meaning that the deepest layer is assumed to be the target layer. Using Eq. (4), the average depth for the target layer is found to be about 4.84 km.

The power values with wavenumbers higher than 0.6 rad/km need not be included in the calculations since they represent shallower underground mass; furthermore, they may affect iterations, causing the calculated model to be inaccurate. In order to remove noise from the data, the data are filtered using a low pass filter. Filtering is done using the software with a cutting wavenumber of 0.258 rad/km.

The Bouguer Anomaly Map of Turkey (MTA, 2006) was computed using a standard Bouguer density value of 2.67 g/cm³. The buried mass at Çumra should have a higher mean density than the standard density of the map. Considering the study area being a remnant of the Tethys Ocean and the high Bouguer values where there are only sediments visible at the surface, we suspect that a possible source for the relatively high Bouguer anomaly is an oceanic rock at a certain depth. Oceanic crust has an average density of 2.9 g/cm³, which is higher than the standard Bouguer density of 2.67 g/cm³, and thus mostly has a positive Bouguer anomaly (Rogers et al., 2008). Considering these differences, the density difference is decided to be slightly higher than the difference between standard density and oceanic crusts' average densities (Dr); therefore it is set as 0.25 g/cm³.

After the average depth and density difference parameters are defined and calculated, the Bouguer anomaly data are processed by the software that we developed. After 10 iterations, if the RMS error between measured and calculated Bouguer anomalies is less than 1%, the calculated layer model is assumed to be acceptable.

The calculated model has a depth range of 4.1 to 5.4 km, having the calculated average depth value 4.84 km as an approximate midpoint. The model consists of many hill structures with kilometers of radii and a few hundred meters of relative heights, which designate an acceptable model (Figure 8). At the center, showing high Bouguer values, there are SE to NW directed structures, fitting the suture zones shown in Figure 1 perfectly. On the other hand, calculated structures surrounding the center of the study area, especially those located at the eastern and southwestern parts of the study area, are resulted from marble and limestone masses that could be observed on the geological map of the area and may not point out an underground structure.

As a poststudy, total extra mass that would result in the measured Bouguer anomaly is calculated using the model. Since the theoretical model is separated into prisms with equal base areas of $1 \times 1$ km², it is possible to calculate their volumes. Firstly, a certain depth is chosen as the base of the hills at the center, which is decided to be 4.9 kilometers for this study (Figure 9). Depths of all the prisms in the model are normalized according to this depth. During the modelling process of the theoretical model, the modelled layer is assumed to have a density difference of 0.25 g/cm³. Multiplying the total volume and density difference of the model would result in total mass difference, which
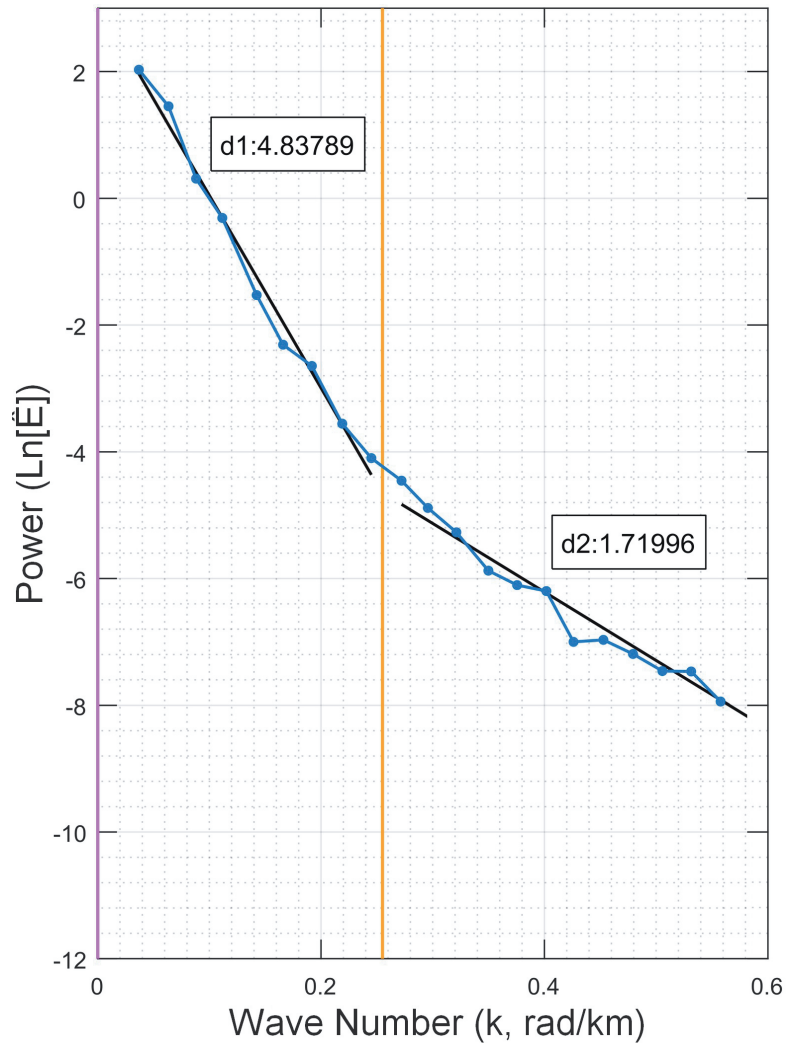
**Figure 7.** Power spectrum plot of the Çumra Bouguer gravity data. The points between magenta and orange vertical lines are used in depth estimation. Average depth of the target layer is about 4.84 km.

in this case points out the unexpected extra mass for the designated area. The extra mass is calculated using depth information of the model calculated for 1088 prisms at the center, and resulting in a total of 67.343 Gt of extra mass.

**6. Discussion**
The Bouguer anomaly map of the study area shows abnormally high values around Çumra, where only Cretaceous clastics are visible at the surface. The high Bouguer anomaly in this region appears to point out an unexpected body emplaced within a homogeneous underground structure (Figure 8). The approximate extra mass caused by the associated body is calculated to be about 67 Gt (Figure 9). This anomalous body is possibly an ophiolite block emplaced during closure of the Tethys Ocean.

The area itself contains several suture zones, marking the area a subduction area as a remnant of the Tethys Ocean (Şengör and Yılmaz, 1981). The geological maps of this area show several areas with ophiolitic rocks, supporting the present study further (Ercan, 1986; MTA, 2002). Since ophiolites are dense oceanic rocks (2.8–3.3 g/cm³), their Bouguer anomalies tend to have positive-directed values whether they are buried under the sediments or cropped out of the surface (Manghnani and Coleman, 1981; Shelton, 1990; Savvaidis et al., 2000; Berlin, 2005). The ophiolite alignment in the area, however, does not seem to affect the anomalies as much as anticipated (Figure 3). The ophiolite outcrop to the west of Konya has an indistinct effect on Bouguer anomalies, which is possibly because of the ophiolite body's not having a deep extent. On the other hand, the outcrop to the south of Çumra appears to have
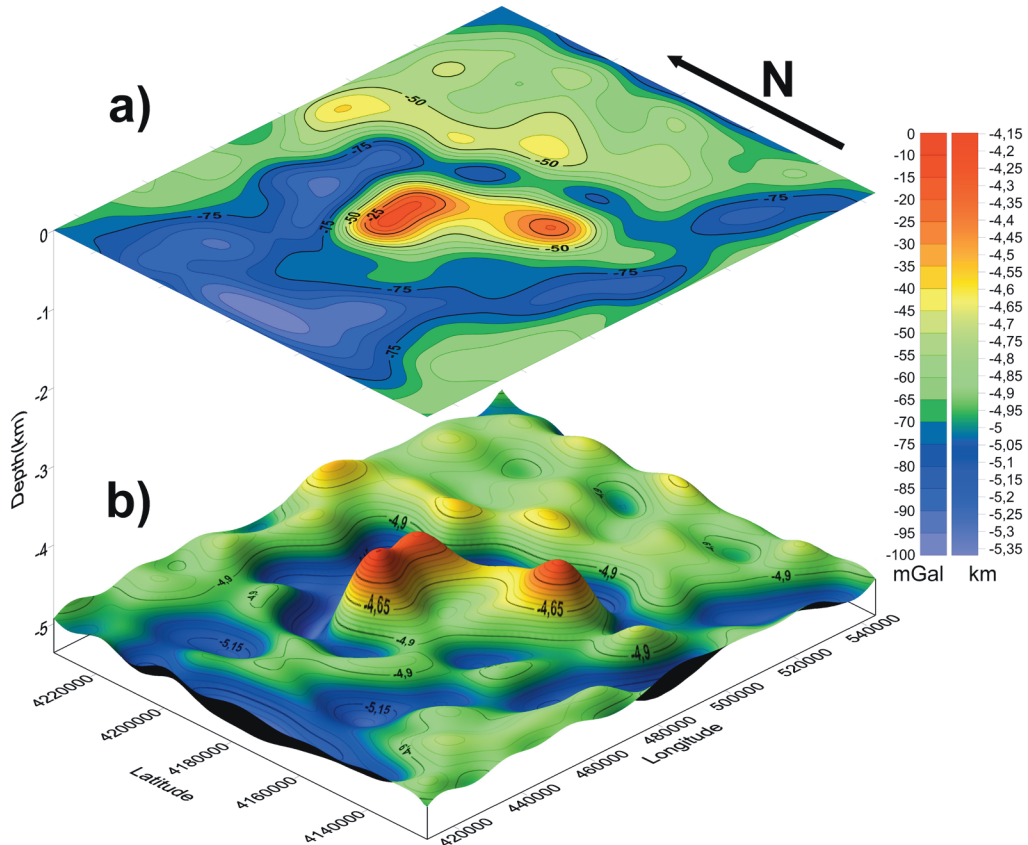
**Figure 8.** a) Filtered Bouguer anomaly data. b) Calculated depth map for the target layer.

a clearer increasing effect on Bouguer anomalies, which can be interpreted as a larger body of ophiolite with a dip towards the southwest from the outcrop.

Aside from high Bouguer gravity anomalies due to their high densities, ophiolites have strong effects on magnetic anomalies due to their high magnetic susceptibilities (Rao et al., 2016). Numerous studies show that ophiolites usually have positive magnetic anomalies (Kane et al., 2005; Dolmaz, 2007; Rao et al., 2016); thus, comparing magnetic and Bouguer gravity anomaly maps of the Çumra area would support the buried ophiolite thesis. An examination of the area's aeromagnetic data points out a strong magnetic anomaly around the Çumra region as seen in Figure 10 (MTA, 2007). Although there are volcanic rocks located to the west, southeast, and east of Konya, they have low wavelength effects on the aeromagnetic map and slight effects on the Bouguer gravity map. On the other hand, the location of the relatively high Bouguer anomaly also appears to have relatively high magnetic anomalies, similarly. Furthermore, the magnitude and wavelength of this anomaly hint that the magnetized body beneath the area is as deep as that interpreted in the Bouguer gravity modelling.

It is known that the Neo-Tethys Ocean closed and the oceanic basin subducted northward during the Lower Miocene period, before the strong volcanic activities and ophiolite emplacements over the Anatolide–Tauride Platform (Okay, 2011). In the Çumra area, which is on the suture zone of this closure, an obducted portion of the basin may have been emplaced over the Anatolide–Tauride Platform by obduction. Up to now, thick sediment layers could have accumulated and covered up the whole area, as well as the ophiolite (Figure 11). In brief, it is acceptable to interpret an obducted portion of an oceanic crust that is possibly laid beneath the thick sediments in the Çumra area, Konya.

## 7. Conclusion
The Çumra area lies on a suture zone remaining from the closing of the Neo-Tethys Ocean (Figure 1). In the Konya Basin to the north of Çumra, there are relatively high Bouguer anomalies despite the area having a flat topography and a sediment cover (Figure 3). Spectral analysis of the anomaly showed that there is an increment of mass at a depth of about 4.84 km (Figure 7). The anomaly is filtered in order to remove the effects of
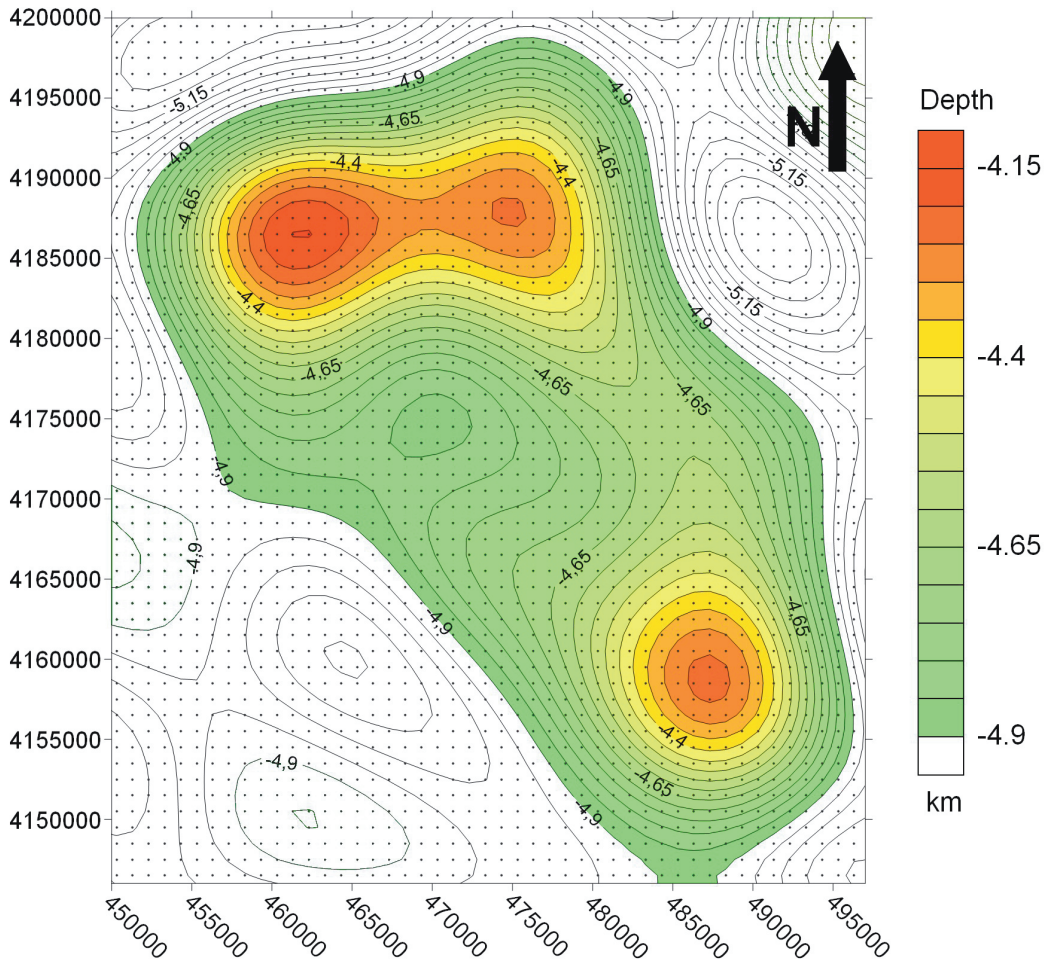
**Figure 9.** Area of the resulted depth map (Figure 8) that is used in extra mass calculations.
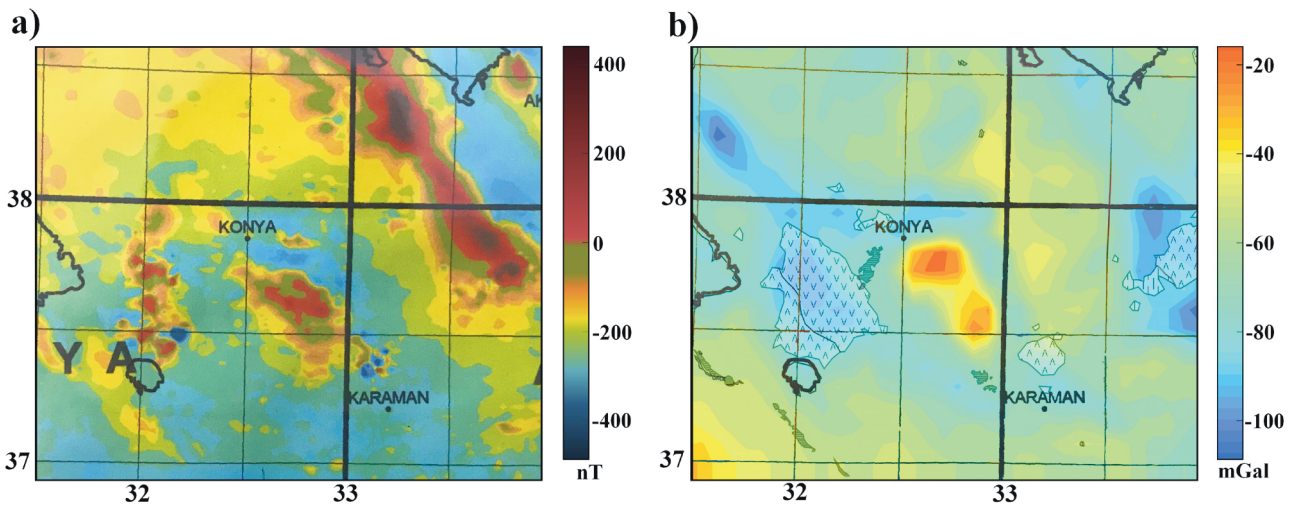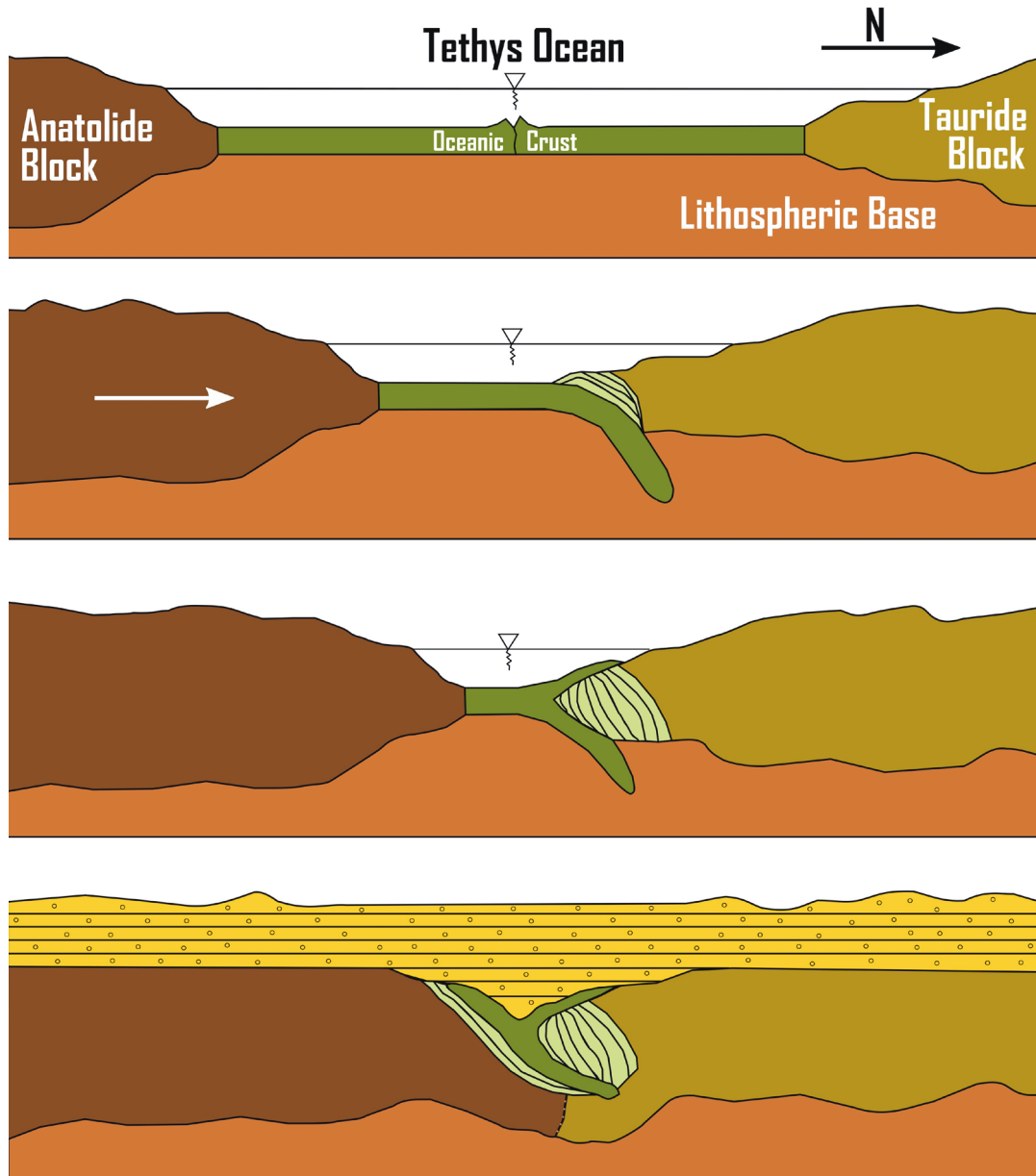


**Figure 10.** a) Aeromagnetic data of the area (MTA, 2007). b) Bouguer data of the area with several volcanics marked. Both maps include lakes marked.

**Figure 11.** Emplacement of an obducted portion of the oceanic crust is schematized. When Tethys Ocean started to close at Lower-Miocene, continental crust bodies (Anatolide and Tauride) squeezed the oceanic crust. During this period, some portion of the oceanic body emplaced over continental crust while the rest subducted beneath lithospheric base. After the ocean totally closed, obducted oceanic body covered with thick sedimentary layers.

the masses shallower than this depth. Then the rough underground geometry of a homogeneous layer with a density difference of 0.25 g/cm³ is modelled using the vertical prisms method (Figure 8). Furthermore, a defined portion of the calculated model that is constructed of identical prisms is used for extra mass calculations and excess mass is found to be about 67 Gt (Figure 9). The possibility of a buried mass of ophiolite, under the sediments, is discussed as the reason for such a high anomaly. Ophiolites are dense rocks and have high magnetic susceptibilities; thus this information supports this thesis considering the Bouguer gravity and magnetic data of the study area with large wavelength and high amplitude anomalies (Figure 10). Modelling studies and interpretations indicate that the possibility of an obducted oceanic crustal block emplaced beneath the Çumra area during the closure of the Neo-Tethys Ocean (Figure 11) is considerable.

## References

Ateş A, Kearey P (1995). A new method for determining magnetization direction from gravity and magnetic anomalies: application to the deep structure of the Worcester Graben. J Geol Soc Lond 152: 561-566.

Banks RJ, Swain CJ (1978). The isostatic compensation of East Africa. Proc R Soc Lond A 364: 331-352.

Berlin M (2005). Tectonic Wedging in the California Coast Ranges: Useful Model or an Unreasonable Hypothesis? GEOL 5690, Tect West U.S.

Büyüksaraç A, Reiprich S, Ateş A (1998). Three-Dimensional magnetic model of amphibolite complex in Taşkesti area, Mudurnu Valley, North-West Turkey. J Balk Geop Soc 33: 44-52.

Cordell L, Henderson RG (1968). Iterative three dimensional solution of gravity anomaly data using a digital computer. Geophysics 33: 596-601.

Dewey JF, Burke KC (1973). Tibetan, Variscan and Precambrian basement reactivation: products of continental collision. J Geol 81: 683-692.

Dolmaz MN (2007). An aspect of the subsurface structure of the Burdur-Isparta area, SW Anatolia, based on gravity and aeromagnetic data and some tectonic implications. Earth Pla Sp 59: 5-12.

Ercan T (1986). Cenozoic volcanism of Central Anatolia. MTA Derg 107: 119-140 (article in Turkish with an abstract in English).

Genç T (1997). Gravite ve Manyetik Yöntemlerde Modelleme. In: Canıtez N, editor. Jeofizikte Modelleme. İstanbul, Turkey: Literatür Yayınları, pp. 57-84.

Hahn A, Kind EG, Mishra DC (1976). Depth estimation of magnetic sources by means of Fourier amplitude spectra. Geop Pros 24: 287-308.

Kane I, Stampolidis A, Tsokas NG, Bushati S, Kondopoulou D, Tsourlos P (2005). The structure of the ophiolitic belt in Albania inferred from geomagnetic anomalies. An Geop 48: 231-246.

Kearey P (1991). A possible source of the South-Central England magnetic anomaly: basaltic rocks beneath the London platform. J Geol Soc Lond 148: 775-780.

Manghnani MH, Coleman RG (1981). Gravity profiles across the Samail Ophiolite, Oman. J Geop Res 86: 2509-2525.

Maus S, Dimri V (1996). Depth estimation from the scaling power spectrum of potential fields? Geop J Int 124: 113-120.

MTA (General Directorate of Mineral Research and Exploration of Turkey) (2002). Geological Maps of Turkey (scale: 1/500000).

MTA (General Directorate of Mineral Research and Exploration of Turkey) (2006). Bouguer gravity anomaly map of Turkey (scale:1/2.000.000). Ankara, Turkey: MTA Pub.

MTA (General Directorate of Mineral Research and Exploration of Turkey) (2007). Aeromagnetic Map (Total Intensity) of Turkey (scale: 1/2.000.000). Ankara, Turkey: MTA Pub.

Nouck PN, Eliezer MD, Mbarga TN, Tabod C (2006). Spectral analysis and gravity modelling in the Yagoua, Cameroon, sedimentary basin. Geof Int 45: 209-215.

Okay AI (2008). Geology of Turkey: a synopsis. Anschnitt 21: 19-42.

Okay AI (2011). Tavşanli zone: the northern subducted margin of the Anatolide-Tauride block. MTA Derg 142: 195-226.

Okay AI, Tüysüz O (1999). Tethyan sutures of northern Turkey. Geol Soc Lond Spec Pub 156: 475-515.

Öksüm E, Etiz A, Dolmaz MN (2005). An attempt to define depth of the structure based on three dimensional (3-D) modeling of gravity anomalies. İstanbul Yerbilimleri Dergisi 18: 219-227 (article in Turkish with an abstract in English).

Parker RL (1972). The rapid calculation of potential anomalies. Geop J R Ast Soc 35: 447-455.

Pawlowski RS, Hansen RO (1990). Gravity anomaly separation by Wiener filtering. Geophysics 55: 539-548.

Rao PB, Radhakrishna M, Haripriya K, Rao BS, Chandrasekharam D (2016). Magnetic anomalies over the Andaman Islands and their geological significance. J Earth Syst Sci 125: 359-368.

Robertson AH, Okay A, Parlak O, Ustaömer T (2009). The Tectonic Setting and Development of the Anatolian Suture Zones: Problems and Possible Solutions. 62nd Geol Kur Turkey, Ankara, Turkey: MTA.

Rogers N, Blake S, Burton K (2008). An Introduction to Our Dynamic Planet. Cambridge, UK: Cambridge University Press.

Savvaidis AS, Tsokas GN, Papazachos CB, Kondopoulou D (2000). A geophysical study of the ophiolite complex and the sedimentary basins ın the northwest part of the Chalkidiki Peninsula (N. Greece). Surv Geop 567-595.

Şengör AMC, Yılmaz Y (1981). Tethyan evolution of Turkey: a plate tectonic approach. Tectonophysics 75: 181-241.

Shelton AW (1990). The interpretation of gravity data in Oman: constraints on the ophiolite emplacement mechanism. Geol Soc Lond Spec Pub 459-471.

Smith A (1971). Alpine deformation and the oceanic areas of Tethys, Mediterranean and Atlantic. Geol Soc Am Bull 82: 2039-2070.

Spector A, Grant F (1970). Statistical models for interpreting aeromagnetic data. Geophysics 35: 293-302.